HILIC-UPLC-MS for high throughput and isomeric N-glycan separation and characterization in Congenital Disorders Glycosylation and human diseases

Angela Messina, Angelo Palmigiano, Francesca Esposito, Agata Fiumara, Andrea Bordugo, Rita Barone, Luisa Sturiale, Jaak Jaeken, et al.

Glycoconjugate Journal
Official Journal of the International Glycoconjugate Organization

ISSN 0282-0080

Glycoconj J
DOI 10.1007/s10719-020-09947-7

Springer

Glycoconjugate Journal
https://doi.org/10.1007/s10719-020-09947-7

ORIGINAL ARTICLE

HILIC-UPLC-MS for high throughput and isomeric *N*-glycan separation and characterization in Congenital Disorders Glycosylation and human diseases

Angela Messina[1] · Angelo Palmigiano[1] · Francesca Esposito[1,2] · Agata Fiumara[3] · Andrea Bordugo[4] · Rita Barone[1,5] · Luisa Sturiale[1] · Jaak Jaeken[6] · Domenico Garozzo[1]

Received: 21 April 2020 / Revised: 7 September 2020 / Accepted: 8 September 2020

Abstract

N-glycan analyses may serve uncovering disease-associated biomarkers, as well as for profiling distinctive changes supporting diagnosis of genetic disorders of glycan biosynthesis named congenital disorders of glycosylation (CDG). Strategies based on liquid chromatography (LC) preferentially coupled to electrospray ionization (ESI) - mass spectrometry (MS) have emerged as powerful analytical methods for *N*-glycan identification and characterization. To enhance detection sensitivity, glycans are commonly labelled with a functional tag prior to LC-MS analysis. Since most derivatization techniques are notoriously time-consuming, some commercial analytical kits have been developed to speed up *N*-deglycosylation and *N*-glycan labelling of glycoproteins of pharmaceutical and biological interest such as monoclonal antibodies (mAbs). We exploited the analytical capabilities of *Rapi*Fluor-MS (RFMS) to perform, by a slightly modified protocol, a detailed *N*-glycan characterization of total serum and single serum glycoproteins from specific patients with CDG (MAN1B1-CDG, ALG12-CDG, MOGS-CDG, TMEM199-CDG). This strategy, accomplished by Hydrophilic Interaction Chromatography (HILIC)-UPLC-ESI-MS separation of the RFMS derivatized *N*-glycans, allowed us to uncover structural details of patients serum released *N*-glycans, thus extending the current knowledge on glycan profiles in these individual glycosylation diseases. The applied methodology enabled to differentiate in some cases either structural isomers and isomers differing in the linkage type. All the here reported applications demonstrated that RFMS method, coupled to HILIC-UPLC-ESI-MS, represents a sensitive high throughput approach for serum *N*-glycome analysis and a valuable option for glycan detection and separation particularly for isomeric species.

Keywords HILIC · High throughput *N*-glycomics · CDG · LC-MS · Oligomannose type *N*-glycans

Angela Messina and Angelo Palmigiano contributed equally to this work.

Electronic supplementary material The online version of this article (https://doi.org/10.1007/s10719-020-09947-7) contains supplementary material, which is available to authorized users.

✉ Domenico Garozzo
domenico.garozzo@cnr.it

[1] CNR, Institute for Polymers, Composites and Biomaterials, IPCB, Catania, Italy

[2] Present address: IOM Ricerca S.r.l, Viagrande, CT, Italy

[3] Pediatric Clinic- Department of Clinical and Experimental Medicine, University of Catania, Catania, Italy

[4] Department of Mother and Child, Pediatric Clinic, University Hospital of Verona, Verona, Italy

[5] Child Neurology and Psychiatry, Department of Clinical and Experimental Medicine, University of Catania, Catania, Italy

[6] Center for Metabolic Diseases, UZ and KU Leuven, Leuven, Belgium

Published online: 11 September 2020

Introduction

N-glycosylation is a major post-translational protein modification that plays a pivotal role in many biological processes including intercellular signaling and recognition. In eukaryotes, *N*-glycan biosynthesis spreads over different cellular compartments. It starts in the cytosol and continues on the cytoplasmic and then the luminal side of the endoplasmic reticulum (ER) where *N*-glycans are assembled and attached to proteins through the amide group of an asparagine (Asn) within an Asn-Xxx- Ser/Thr sequon, with Xxx different from proline. Subsequent processing and modification of *N*-glycan structures form a huge variety of glycoforms in the Golgi apparatus [1, 2].

The glycan moiety of glycoproteins strongly impacts on their physiochemical properties (such as protein folding, half-life, solubility) and biological functions (such as receptor recognition, immunological regulation, intercellular signaling). Therefore, detailed structural characterization of glycans is essential to understand physiological processes and to correlate alterations in glycan structures with various pathological conditions such as cancer [3, 4], neurodegeneration [5–9], autoimmune diseases [10, 11] or genetic defects such as congenital disorders of glycosylation (CDG) [5, 12–15].

CDG are characterized by hypoglycosylation usually due to defective *N*-glycan biosynthesis. The first-line CDG diagnostic test is serum transferrin glycoform analysis by isoelectric focusing, capillary electrophoresis or mass spectrometry [15]. CDG-I refers to glycan assembly defects in the cytosol-endoplasmic reticulum, leading to underoccupancy of transferrin *N*-glycosylation sites with missing entire glycan chains (type 1 pattern). In CDG-II, transferrin has truncated oligosaccharide chains due to abnormal glycan processing in the Golgi apparatus (type 2 pattern). More than 130 CDG have been reported [16, 17]. They are clinically heterogeneous diseases with mostly major nervous system involvement and variable extra-neurological symptoms (hepatopathy, endocrinopathy, immunodeficiency, coagulopathy, a.o.). Patients with CDG usually have thus a severe disability burden and, on the other hand, CDG are a unique natural model to study the link between defective glycosylation and disease pathomechanisms. This insight may help to understand acquired *N*-glycosylation changes in common multifactorial diseases such as neurodegenerative diseases and cancer.

Major advances in analytical methodologies for *N*-glycosylation analysis have been made in recent years [18, 19], and several tailored strategies combining mass spectrometry with liquid chromatography separation (LC-MS) are now available for glycan characterization [20]. High throughput (HT) *N*-glycomics profiling are largely performed by hydrophilic-interaction ultra high performance liquid chromatography with fluorescence detection (HILIC-UPLC-FLD) [21–23], by multiplexed capillary gel electrophoresis with laser-induced fluorescence detection (CGE-LIF) [24] or by matrix-assisted laser desorption/ionization tandem time-of-flight MS (MALDI TOF/TOF MS/MS) [23]. A HT HILIC-LC-MS method, enabling identification either by retention times and by molecular mass measurements, with accuracy at the ppm level, has been previously set-up for glycosaminoglycan oligosaccharides [25, 26], but a similar method for *N*-glycan analysis is currently missing [27], although very recently a nice HT method using porous graphitized carbon LC-MS enabling *N*- and *O*- glycomic was presented [28].

To meet the needs of the pharmaceutical industry, some kits dedicated to the HT LC-MS analysis of *N*-glycans released from monoclonal antibodies (mAb) have recently been introduced. They take advantage of the high availability of mAb glycosylation sites that can be easily deprived in a few minutes from their *N*-glycan moieties by the action of peptide-*N*-glycosidase F (PNGase F). These commercial tools rely on derivatization of the released *N*-glycans with a labelling fluorophore, such as procainamide (ProA) [29, 30] or *Rapi*Fluor-MS reactant (RFMS) [31]. The latter contains a positively charged tertiary amine, thus increasing ionization efficiency in positive ion mass spectrometry.

N-glycan labelling exploits the reaction rate between the glycosylamine group at the reducing end, generated by PNGase F digestion, and a *N*-hydroxysuccinimidyl (NHS) carbamate reacting group [31–33]. The deglycosylation step should necessarily be very fast (usually five minutes at 50 °C), since glycosylamine at such temperature has a half-life of approximately 2 h [31]. This reaction underlines the tagging step of the *Rapi*Fluor protocol to investigate the *N*-glycan repertoire of monoclonal antibodies, which glycosylation sites are easily accessible from PNGase owing to their conformational features. Our purpose was to extend the applicability of such HT method to different and more complex systems as serum, cerebrospinal fluid and tissues, to uncover glycosylation changes in human diseases and possible targets for future glyco-based therapies. However, because of the high heterogeneity of many biological substrates also comprising glycoproteins in very low amount, we set-up and optimized a non-conventional *Rapi*Fluor protocol, by prolonging denaturation and deglycosylation time up to 60 min, so as to obtain wide-ranging and reproducible glycosylation profiles without any loss of information.

Another important aspect is the HT capability of the *Rapi*Fluor kit, supporting the analysis of batches of 24 samples up to 96 samples in a single run.

Here we present our more representative data regarding serum *N*-glycan analysis of some patients with CDG as a reliable and innovative example for sera HT analysis in health and disease. This strategy joins chromatographic separation and high-accuracy molecular mass determination, providing further structural insights compared to the traditional approaches, such as the differentiation of isomeric *N*-glycan structures.

Materials and methods

Serum samples were collected from 3 patients with (Man1B1-CDG, MOGS- CDG, and ALG12- CDG, respectively) and 2 patients with TMEM199-CDG in the context of pertinent clinical investigations. Demographic, clinical and molecular characteristics of patients with CDG are reported in Supplementary Table 1. Serum control samples were from healthy subjects age and sex matched as the patients which underwent blood sampling for routine blood check-up. Written informed consents for the study analyses were obtained from all participants and/or their parents.

7.5 microliters of serum from MAN1B1-CDG, MOGS-CDG, TMEM 199-CDG and ALG12-CDG patients, were used for *N*-glycan profiling. The same volume of diluted IgG was adopted to profile IgG from MOGS-CDG. IgG was isolated from serum (120 µL) by immunoaffinity separation with IgG (Fc) Depletion Column pre-packed with anti-IgG IgY beads (GenWay Biotech, San Diego, CA, USA), as previously described [34]. 1 µL of the extracted IgG containing solution was diluted 1:10 in phosphate-buffered saline, whose portion of 7.5 µL was analyzed. Enzymatic release and labelling of *N*-glycans were performed by the GlycoWorks *Rapi*Fluor-MS *N*-Glycan kit (Waters Corporation, Milford, MA, USA), modifying the suggested protocol by increasing deglycosylation time from 5 to 60 min. Since *N*-glycosylamine readily converts to a reducing-end sugar with a half-life of approximately 2 h at 50 °C [31], we tested such reaction at the same temperature over different reaction times: 5, 60, 90, 120 and 300 min (data not shown), concluding that 60–90 min was the optimal range for *N*-glycan recovering from the analyzed samples (sera, cerebrospinal fluids and mouse brain tissues) as expected. Total sample preparation time was about 2 h. All the reaction and purification steps were carried out in the 96 well plate GlycoWorks Kit. Labelled *N*-glycans, tagged at the glycosylamine residue of the terminal chitobiose epitope [20, 33], were separated by an UHPLC THERMO system (Ultimate 3000 LPG3400SD) coupled to an Exactive Orbitrap HESI-II mass spectrometer (Thermo Fisher Scientific Inc., Bremen, Germany). Samples were analyzed by a hydrophilic interaction liquid chromatography (HILIC) column (ACQUITY UPLC Glycan BEH Amide 130 Å, Waters, 2.1 mm × 150 mm, 1.7 µm, Waters Corporation Milford, MA, USA). The separation was carried out at a flow rate of 0.4 ml/min at 60 °C, with a mobile phase A consisting of 50 mM ammonium formate aqueous solution (pH 4.4) and a mobile phase B as pure ACN (acetonitrile). A mobile phase A gradient ramping from 25 to 46% over 35 min was used.

MS analyses were conducted under the following conditions: heater temperature 375 °C, capillary temperature 120 °C, spray voltage 1.90 kV, capillary voltage 120 V, tube lens voltage 120 V, skimmer voltage 50 V. Spectra were acquired in positive polarity, and resolution was adjusted at 70,000 FWHM @200 m/z.

We performed three technical replicates of each sample and three runs of each analysis (for a total of nine chromatograms for a single disease) and we found not substantial differences between chromatograms and spectra recorded.

Raw files were uploaded to Glycopost (GPST000114 https://glycopost.glycosmos.org/).

Data analysis

Chromatographic retention times were compared with that reported in glycostore (https://glycostore.org/waters).

N-glycan species were identified by using bioinformatics tools, such as GlycoMod (http://web.expasy.org/glycomod/), Glycoworkbench v2.1 [35] and by tools provided by the.

Consortium for Functional Glycomics (CFG).

Results and discussion

MAN1B1-CDG (alpha 1,2-mannosidase deficiency, OMIM 604,346).

MAN1B1 encodes the α1,2 mannosidase that generates Man-8 D1D3 (also known as $Man_8GlcNAc_2$ isomer B) by catalyzing the deletion of the first mannose residue from the middle branch of $Man_9GlcNAc_2$ (Man-9), as depicted in Scheme 1a. MAN1B1-CDG, the most common CDG-II, is mainly characterized by intellectual disability, facial dysmorphism (such as flat oval face, low frontal hairline, hypertelorism, downslanting palpebral fissures, prominent nose tip, large low-set ears and thin upper lip), macrocephaly and truncal obesity [36, 37].

MAN1B1-CDG *N*-glycosylation, including total serum and single glycoproteins, such as transferrin, Immunoglobulin G (IgG) and alpha1-antitrypsin (α1AT), has been widely studied. Rymen et al. [36] first reported that MAN1B1 deficiency causes a CDG-II with accumulation of hybrid *N*-glycans and noticeable increase of $Man_6GlcNAc_2$ (Man-6) in serum. They also demonstrated that the MAN1B1 capability to trim Man-9 to Man-8 was delayed in patient fibroblasts. Van Scherpenzeel et al. [37] performed *N*-glycosylation studies by direct analysis of intact serum transferrin, IgG and α1AT by high resolution ESI-MS and reported an increase of hybrid (fucosylated and unfucosylated) *N*-glycans in all the glycoproteins. Saldova et al. [38] investigated serum and IgG *N*-glycosylation by HILIC-UPLC-FLD and successive exoglycosidase digestions and reported increasing amounts of hybrid and oligomannose N-glycan structures and of antennary fucosylated *N*-glycans bearing the sialyl-Lewis X (sLe^x) epitope. Duvet et al. [39] used endoglycosidase H (Endo H) to release *N*-glycans from serum proteins exploiting the ability of this enzyme to

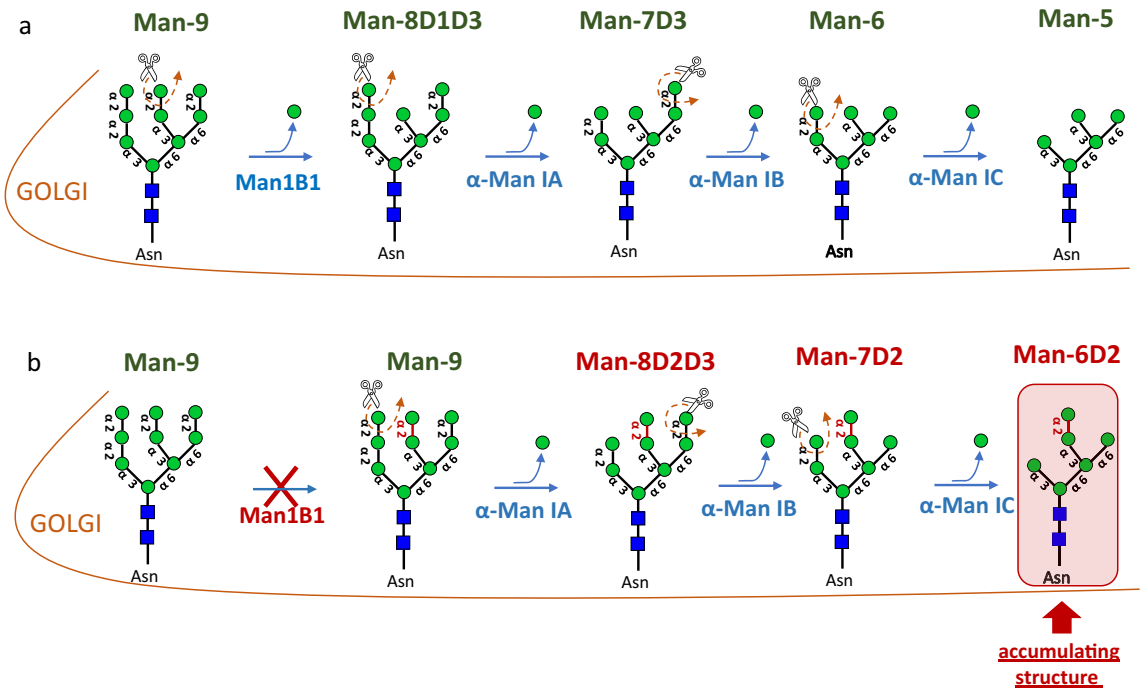

Scheme 1 Schematic representation of the MAN1B1 defect in the *N*-linked glycan biosynthetic pathway (a). The corresponding streamlined part of the normal biosynthetic pathway is reported in (b) consistent with major *N*-glycan species present in controls. Deficiency of α(1,2)-mannosidase (MAN1B1) leads to Man-6D2 isomer accumulation: besides an absent removal of the terminal mannose residue from the middle branch of $Man_9GlcNAc_2$ due to MAN1B1-deficiency, the following mannosidases (Golgi α-mannosidase IA, IB and IC) continue their activity, removing a α(1,2)-bound mannose moiety from A- and C- branches. Glycan symbols: GlcNAc, blue square; Man, green circle

selectively deglycosylate oligomannose and hybrid type *N*-glycans from serum glycoproteins. By subsequent alpha-mannosidases treatments of the Endo H released *N*-glycans, they demonstrated that the accumulating hybrid *N*-glycan in MAN1B1-CDG have isomeric structures different from those present in control serum samples [39]. Recently, Barbosa et al. [40] applied an improved MS protocol for relative quantification of *N*-glycans also to MAN1B1-CDG.

To get more information on the possible occurrence of aberrant isomeric structures we analyzed, by our *Rapi*fluor-based UHPLC-MS, a serum sample of a patient with MAN1B1 deficiency. Although the above mentioned studies led to a better understanding of the molecular defect in MANB1-CDG, some unclarified issues remain. The most important one is whether in MAN1B1-CDG serum, oligomannose *N*-glycans retain the same isomeric structures as present in normal serum proteins. Our modified *Rapi*Fluor method could help to better understand this crucial issue. The extracted ion chromatograms (EICs) of the species corresponding to the oligomannose *N*-glycan series in the patient and in a control are reported in Fig. 1a and b respectively. Chromatographic peaks corresponding to Man-5 and Man-9, share the same unique retention times in patient and control. Contrary to what one would expect (see scheme 1), peaks matching Man-6, Man-7 and Man-8 differ in their retention times and in their relative abundance. In the control sample, the most abundant components were found at 20.4 min (Man-6), 23.7 min (Man-7) and 26.6 min (Man-8) (see Fig. 1b), and their structural assignments were associated with the conventional isoforms in the normal biosynthetic pathway (Scheme 1a). In MAN1B1-CDG, the principal chromatographic ions related to these same species were found at different retention times, i.e. 20.1 min, 23.2 min and 26.3 min for Man-6, Man-7 and Man-8, respectively (see Fig. 1a). Based on the molecular defect, it may be supposed that the corresponding structures in this case match the abnormal isomers, all maintaining the α1,2-terminal mannose at the B branch, indicated in the Scheme 1b as Man6-D2, Man-7D2 and Man-8D2D3 (red labels) [41].

Moreover, it is worth to note that the MAN1B1-CDG chromatographic profile in Fig. 1a, normalized to 100% intensity, is by far dominated by Man-6D2 which showed a much higher relative intensity with respect the other oligomannose *N*-glycan structures. This important finding proved the accumulation of this aberrant glycoform in the patient biosynthetic pathway.

Duvet et al. [39] also demonstrated that the accumulating hybrid $NeuAc_1Gal_1Man_5GlcNAc_3$ glycoform in patients with MAN1B1-CDG, has a peculiar aberrant structure, with the α1,2 mannose residue at the unbranched α1,6-Man arm [39]. Our alternative strategy supports this finding. The EIC of the species at *m/z* 1101.924, corresponding to the

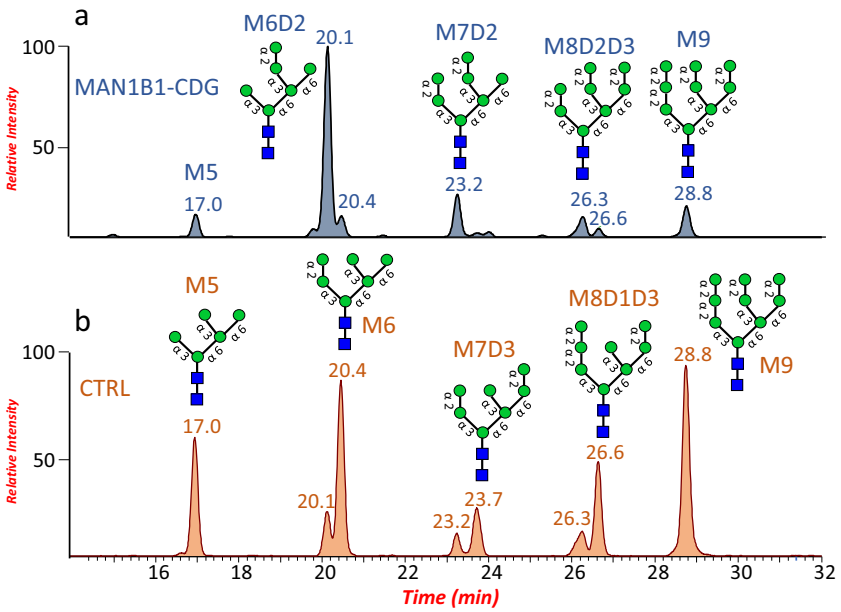

Fig. 1 Extracted Ion Chromatograms (EICs) of the *Rapi*Fluor-MS labelled oligomannose serum *N*-glycans Man_{5-9}-$GlcNAc_2$ from MAN1B1 deficient patient (**a**) compared to the control (**b**). Figure 1a highlights the occurrence in MAN1B1-CDG of Man-6D2 (RT 20.1 min), presenting the sixth mannose linked to the central branch, Man-7D2 (RT 23.2 min), presenting the seventh mannose linked to the B branch, and Man-8D2D3 (RT 26.3 min), presenting the eighth mannose on the C branch [41]. Nevertheless, peaks corresponding to Man-5 (RT 17.0 min) and Man-9 (RT 28.8 min) present the same shapes and are attributed to the same oligomannose *N*-glycan structures in the MAN1B1 deficient patient (a) and control (b). Control *N*-glycan structures were assigned basing on the knowledge of the biosynthesis pathway and according to an earlier HPLC-based study on serum glycoproteins [42]. Glycan symbols: GlcNAc, blue square; Man, green circle

*Rapi*Fluor-MS labelled $NeuAc_1Gal_1Man_5GlcNAc_3$ hybrid *N*-glycan, and of the species at *m/z* 1174.953 corresponding to the fucosylated analog, are reported in Fig. 2a and b for MAN1B1-CDG and control serum. The hybrid *N*-glycans at *m/z* 1101.924 show different retention times (25.3 min and 25.8 min in MAN1-CDG and control, respectively)

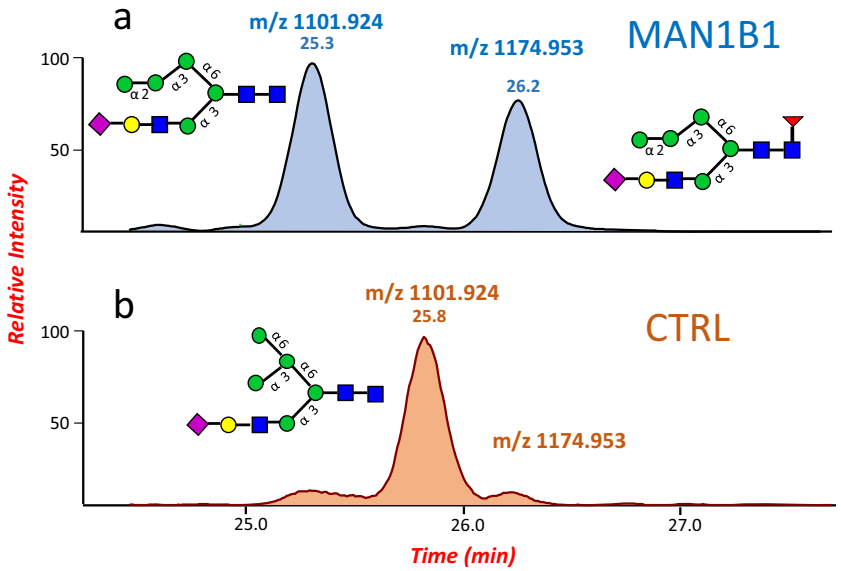

Fig. 2 Extracted Ion Chromatograms (EICs) of *Rapi*Fluor-MS labelled hybrid *N*-glycan isomers in MAN1B1-CDG (**a**) and in a control (**b**). As showed in (a) the hybrid glycan bearing five mannose units, corresponding to the extracted ion current chromatograms at *m/z* 1101.924, has been identified as the hybrid configurations possessing an α1,2-terminal mannose residue, different from the canonical structure reported in the control (b). The corresponding fucosylated peak at *m/z* 1174.953 follows the same pattern, with α-1,3 lacking terminal mannose. A fucosylated hybrid *N*-glycan isomer has not been detected in the control serum (b). Glycan symbols: GlcNAc, blue square; Man, green circle; Gal, yellow circle; NeuAc, purple lozenge; Fuc, red triangle

depending on their different isomeric structures, whereas the fucosylated counterpart at *m/z* 1174.953, is two order of magnitude less in control serum and accumulates only in MAN1B1-CDG.

A list of the stuctures described here with calculated and observed *m/z*, retention times and composition is shown as Supplementary Table 2, while the mass chromatogram is reported in Supplementary Fig. 1.

As a whole the present study applied a modified MS analytical procedure based on *Rapi*Fluor-MS labelled detection of total serum *N*-glycans in MAN1B1-CDG. We first show that this method allows to unravel abnormal oligomannose *N*-glycan structures. We thus could support previously recognized glycoforms in MAN1B1-CDG and identify novel ones.

MOGS-CDG (mannosyl-oligosaccharide glucosidase deficiency, OMIM 606,056).

MOGS-CDG is caused by variants in *MOGS* leading to mannosyl-oligosaccharide glucosidase (MOGS) deficiency. To date, seven patients from five families have been reported [43, 44]. Common clinical features include facial dysmorphism (short palpebral fissures, long eyelashes, broad nose, high arched palate, retrognathia), severe psychomotor disability, epilepsy and hypoimmunoglobulemia with or without recurrent infections. Sadat et al.. [44] found in two affected siblings the oligomannose $Glc_3Man_7GlcNAc_2$ *N*-glycan in IgG and $Glc_3Man_{7-9}GlcNAc_2$ *N*-glycans in serum and skin fibroblasts.

We applied our modified *Rapi*Fluor analysis to investigate the glyco-phenotype in a patient with MOGS-CDG. The superimposed total ion current chromatograms (TICCs) of the IgG released *N*-glycans in serum from the patient and from a control is shown in Fig. 3. The occurrence of $Glc_3Man_7GlcNAc$ and of hybrid glycans is evident in the patient with MOGS-CDG (see red circles). Figure 4 reports the EICs of the accumulating IgG *N*-glycans in the patient, at *m/z* 939.872, 1012.901, 1020.898, 1093.927, 1101.924 and 1174.953, corresponding to the whole set of fucosylated and unfucosylated hybrid structures including glycoforms bearing one, two and three mannose residues at the branched arm. The same species, which are naturally present in control serum, are nearly absent in control IgG (we found only the ion at 21.4 min, consistent with the fucosylated mono-antennary glycoform, with a two orders of magnitude lesser intensity, data not

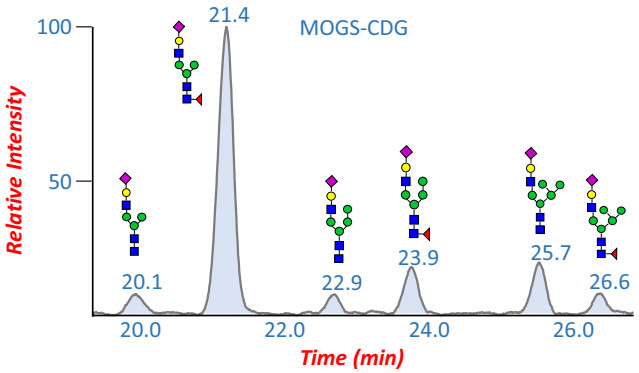

Fig. 4 Extracted ion chromatograms (EICs) of the *Rapi*Fluor-MS labelled fucosylated and unfucosylated hybrid *N*-glycans identified in serum IgG *N*-glycome of a patient with MOGS-CDG. Mannose linkages for the peaks at 22.9 and 23.9 minutes were determined by comparison with serum control (not shown). Glycan symbols: GlcNAc, blue square; Man, green circle; Gal, yellow circle; NeuAc, purple lozenge; Fuc, red triangle

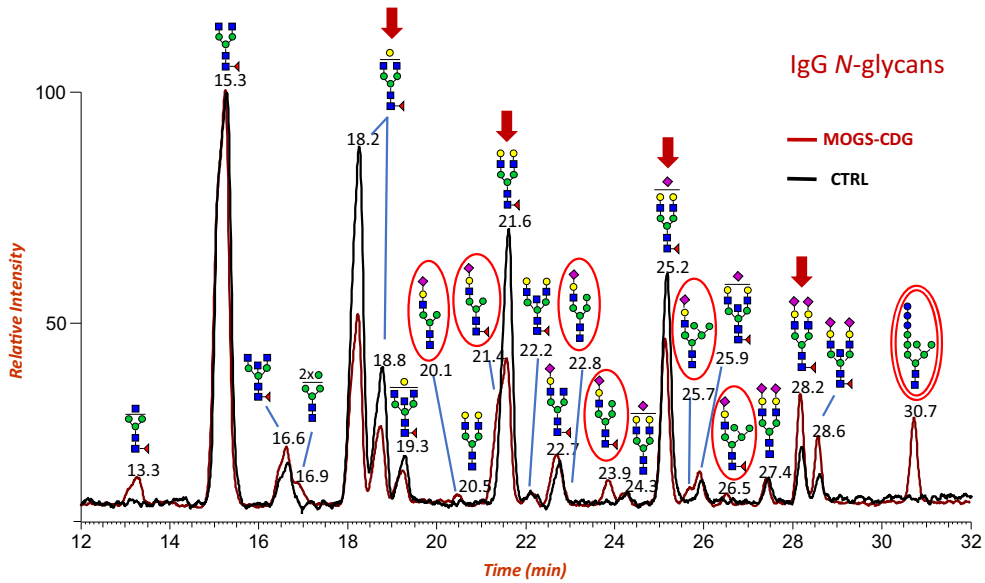

Fig. 3 Overlaid Total Ion Current Chromatograms (TICCs) of *Rapi*Fluor-MS labelled IgG *N*-glycans from a patient with MOGS-CDG (red line) and control (black line). Major changes of specific glycoforms are noted in patient profile by red arrows. The presence of disease-specific oligomannose *N*-glycan biomarkers ($Glc_3Man_7GlcNAc_2$) is highlighted with a double red circle. Single red circles point out the occurrence of extra peaks in patient IgG *N*-glycome corresponding to fucosylated and unfucosylated hybrid structures. Glycan symbols: GlcNAc, blue square; Man, green circle; Gal, yellow circle; Glc, blue circle; NeuAc, purple lozenge; Fuc, red triangle

shown). Assignments were made by comparing chromatographic retention times and *m/z* values. We also observed a decrease of four abundant IgG glycoforms, such as the (two) core-fucosylated biantennary mono- (at 18.2 min and 18.8 min) and di-galactosylated (at 21.6 min) structures, and the core-fucosylated biantennary monosialo- (at 25.2 min) and disialo- (at 28.2 min) *N*-glycans, as indicated in Fig. 3 by red arrows.

The TICC of serum *N*-glycans further supported the patient glycosylation defect, showing besides the hybrid glycans already identified in the isolated IgG, the occurrence of the three peculiar oligomannose structures with composition $Glc_3Man_{7-9}GlcNAc_2$ (Supplementary Fig. 2), as reported [44]. The EICs of these accumulating species at *m/z* 1178.942 (12-saccharide), *m/z* 1259.968 (13-saccharide) and *m/z* 1340.995 (14-saccharide) are reported in Fig. 5. In particular, the two *N*-glycans Glc_3-Man_7-$GlcNAc_2$ and Glc_3-Man_9-$GlcNAc_2$ (Fig. 5a and c) eluted each as a single peak, corresponding to a unique structure, at retention times of 30.8, and 34.0 min respectively, whereas Glc_3-Man_8-$GlcNAc_2$ elution generated two peaks at 32.3 and 32.7 min, attributable to the *N*-glycan isomers differing in the position of the terminal mannose residue at the branched arm (Fig. 5b, mannose linkages not determined).

A list of *N*-glycans found in MOGS-CDG IgG and serum (with calculated and observed *m/z*, retention time and composition), is reported in Supplementary Tables 3 and 4.

TMEM199-CDG (transmembrane protein 199 deficiency, OMIM 616,815).

TMEM199-CDG is a CDG-II. Patients present a mild phenotype of hepatic steatosis. Transferrin mass spectrometry showed an increase of hyposialylated species and also the occurrence of hypogalactosylated glycoforms [45, 46]. The TICC of serum *N*-glycans from two unrelated TMEM199 deficient patients, including a previously reported patient (c.40G > C / c.376-1G > A) [47], and a new patient (c.92G > C) confirmed these results, revealing the same abnormal chromatographic profile with differences in the relative intensity of the biantennary truncated species lacking sialic and/or galactose residues (Supplementary Figs. 3 and 4). The joint EICs of species at *m/z* 1267.985, 1121.438 and 1041.411 corresponding to the disialo-biantennary structure, to the monosialo- and to the monogalacto-, monosialo-biantennary structures respectively, are reported in Fig. 6. Peak assignments were based on the retention behaviour of sialylated *N*-glycans upon HILIC separation, as previously reported [20, 48, 49]. The ion at *m/z* 1041.411 was split in two signals at RT 21.1 and 21.8 min, due to the occurrence of asymmetric isomers at α1–3 or α1–6 mannose branch, with the ion at RT 21.8 min about 6-fold more intense in patient 1 (green line), about 2-fold more intense in patient 2 (red line) and the isomer ion at RT 21.1 min not detected in control EIC. The monosialo-glycan at *m/z* 1122.438, eluted at RT 24.4 min as unique peak, which was found increased by about 3-fold in patient 1 and 2-fold in patient 2. Finally, the biantennary disialo-glycans at *m/z* 1267.985 was separated giving rise to two major sialo-linkage isomers with the structure containing the α2–3 linked sialic acid less retained than the α2-6-linked counterparts [20, 48, 49]. The obtained chromatographic profiles, normalized to 100% intensity with respect to the dominant biantennary fully sialylated structure, enabled a semi-

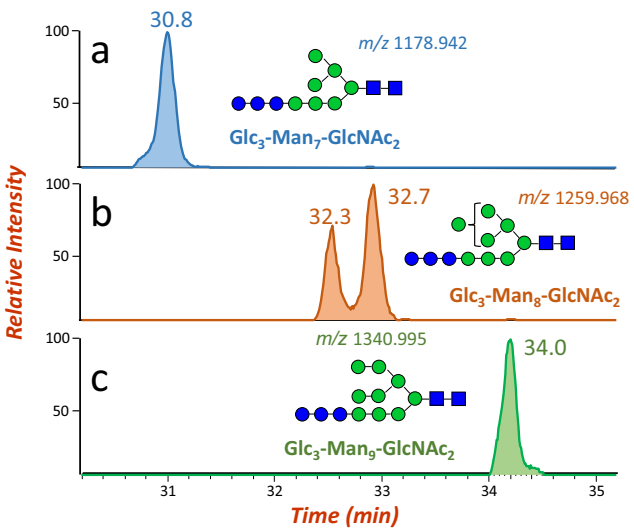

Fig. 5 Extracted ion chromatograms (EICs) of the *Rapi*Fluor-MS labelled Glc_3-Man_{7-9}-$GlcNAc_2$ in MOGS-CDG serum. Glycan symbols: GlcNAc, blue square; Man, green circle; Glc, blue circle

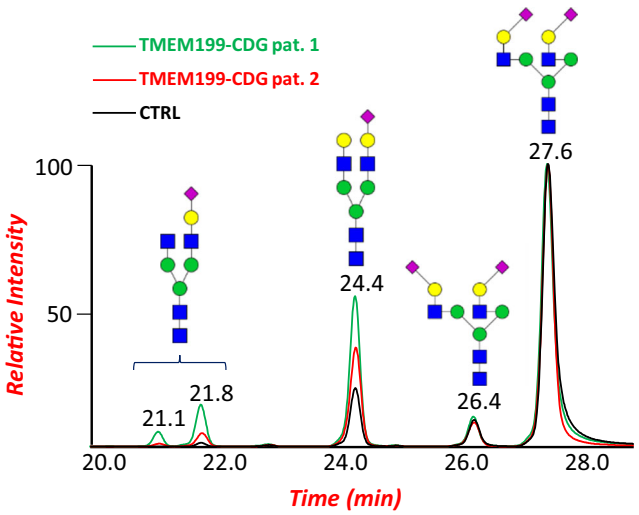

Fig. 6 Extracted ion chromatograms (EICs) of major *Rapi*Fluor-MS labelled biantennary and sialylated *N*-glycans identified in serum of patient 1 with TMEM199-CDG (green line), patient 2 with TMEM199-CDG (red line) and control (black line). Disialo-isomers eluted at RT 27.6 and 26.4 min depending on NeuAc linkage positions, monosialo-biantennary species eluted at RT 24.4 min whereas monogalacto-monosialo- isomers, if present, eluted at two different retention times due to differential Gal-NeuAc elongation at the two branches, respectively. Glycan symbols: GlcNAc, blue square; Man, green circle; Gal, yellow circle; NeuAc, purple lozenge (+ 45°: α2–6 linked; -45°: α2–3 linked; vertical linkage: unassigned)

quantitative comparison between the affected patients, detecting the reduced incorporation of galactose and sialic acid. Further studies are necessary to establish if these differences reflect the severity of the patient glyco-phenotypes, their different genotypes or both.

A list of *N*-glycans found in the serum of the two patients with TMEM199-CDG is shown as Supplementary Tables 5 and 6.

ALG12-CDG (ALG12 α1,6-mannosyltransferase deficiency, OMIM 607,143).

ALG12-CDG is a severe multisystem disease. *ALG12* encodes alpha-1,6-mannosyltransferase (EC:2.4.1.260) that attaches the eighth Man residue to the dolichol-PP-oligosaccharide precursor required for protein *N*-glycosylation. Therefore, in ALG12-CDG the decreased synthesis of the completed glycan precursor containing 14 monosaccharides (Glc_3-Man_9-$GlcNAc_2$) limits its transfer by the oligosaccharyl-transferase complex (OST) to the protein, leading to underoccupancy of protein glycosylation sites (CDG-I). Nine patients with ALG12-CDG have been reported [50–57]. A peculiar feature are severe and recurrent infections associated with hypogammaglobulinemia and B cell dysfunction [50, 52, 53, 55].

The *Rapi*Fluor HILIC UHPLC ESI MS study of an ALG12-CDG deficiency patient (reported in Supplementary Fig. 5) has been recently reported by our group [57], providing additional information on the molecular defect that concerns either the assembly of the dolichol-bound oligosaccharide (CDG-I) and also, unexpectedly, the dysregulation of Golgi processing (CDG-II). ALG12-CDG and MAN1B1-CDG have in common the occurrence of abnormal hybrid *N*-glycans (see Supplementary Fig. 6) besides abnormal oligomannnose serum *N*-glycans [39, 57]. Here we compared the EICs of the oligomannose *N*-glycan structures from Man-5 to Man-8 in patients affected by MAN1B1-CDG, ALG12-CDG and in a control (Fig. 7) to focus on differences between the isomeric glycoforms associated with these diseases. Eleven different oligomannose *N*-glycan structures (three Man-5, three Man-6, three Man-7 and two Man-8) are clearly distinguishable in ALG12-CDG showing the high potential of the methodology. To be noted that the ratio between Man9 (26.6 min) and Man5 (17.0 min, canonical structure) is rather constant in the control in MAN1B1-CDG and in ALG12-CDG, suggesting a further control role for Man5.

A list of *N*-glycans found in ALG12-CDG serum with calculated and observed *m/z*, retention times and composition is shown as Supplementary Table 7.

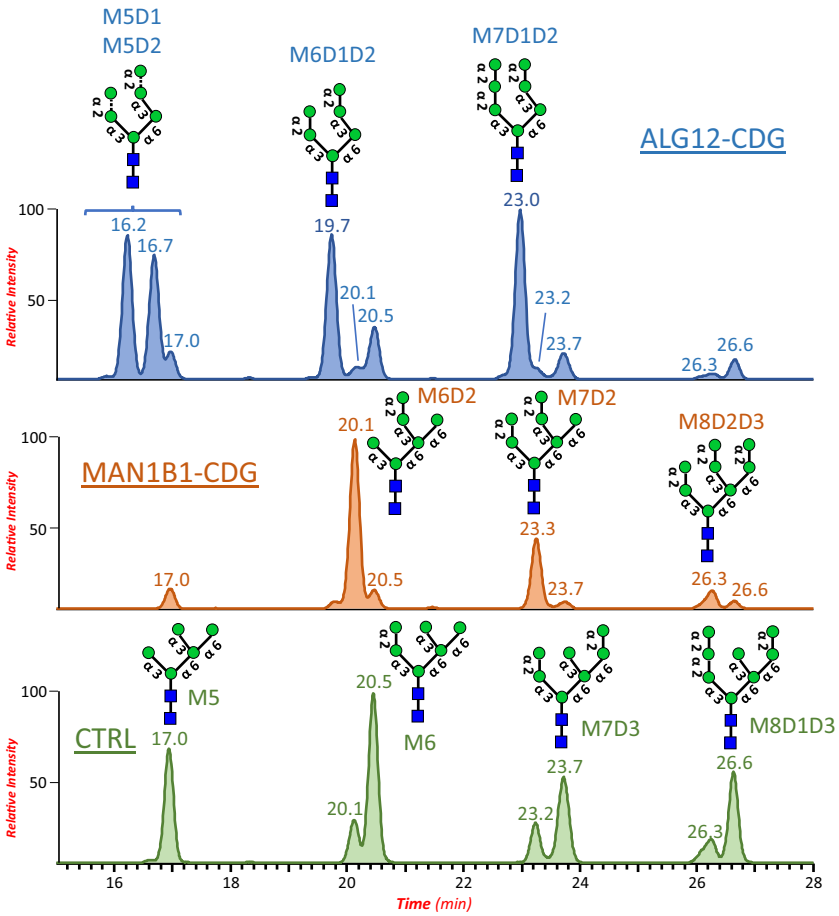

Fig. 7 Comparison of the extracted ion chromatograms (EICs) of the *RapiFluor*-MS labelled oligomannose serum *N*-glycans $Man_{5-9}GlcNAc_3$ from a patient with ALG12-CDG (blue chromatogram), a patient with MAN1B1-CDG (orange chromatogram), and a healthy control (green chromatogram). Dotted lines refer to linkages that should be missing in the final structure. GlcNAc, blue square; Man, green circle

Conclusions

CDG has been considered the paradigm of the glycosylation syndromes, being an extremely diversified group of diseases caused by the inherited defective synthesis of the sugar component of glycoconjugates. Therefore, the utilization of a MS-based HT tool, as here reported, could serve either as a wide screening test to help CDG diagnosis and evaluation, and as a reference point to investigate common diseases implying secondary glycosylation abnormalities.

The present method has the extraordinary ability to provide, in HT, additional structural information otherwise missed. As a proof, we recognized all the previously reported features characterizing the abnormal serum glycosylation of MAN1B-CDG1 deficient patients investigated by MS techniques, such as MALDI TOF of permethylated *N*-glycans, high resolution electrospray MS of isolated proteins, HILIC-UPLC-FLD followed by subsequent exoglycosidase digestions, or by coupling MALDI TOF of permethylated glycans with enzymatic endo-glycosydases. In addition, we extended the current knowledge on specific MAN1B1 glycosylation abnormalities by detecting aberrant isomeric oligomannose *N*-glycan structures in patient serum.

In MOGS-CDG the *Rapi*Fluor ESI-MS approach enabled the identification of a series of unreported hybrid *N*-glycans, both in total serum and in IgG profiles. Moreover, two accumulating structures with composition $Glc_3Man_8GlcNAc_2$ were differentiated. This case highlights how this novel approach might assist the uncovering of novel diagnostic glycans in various CDG-II.

The two studied patients with TMEM199-CDG, displayed abnormal serum glycosylation profiles with increased amounts of hyposialylated and hypogalactosylated structures, associated to this disease, differing in their relative abundance. Although such truncated glycoforms shared the same retention times and therefore the same structures with the control, this approach allowed us to distinguish asymmetrically substituted isomers with different elongation at the α1–3 or α1–6 arm and also isomers differing in α2–3 and α2–6 sialylation, providing a valuable glyco-analytical tool for these investigations.

Also the results obtained in MAN1B1-CDG and ALG12-CDG, show the striking ability of this method in the separation of oligomannose *N*-glycans.

The achievements obtained by coupling HILIC-UPLC with MS, could be further implemented by adopting MS/MS techniques, thus improving the capability of the method for structural investigation in clinical glycan analysis.

Acknowledgements Partial financial support from the association Vaincre le Maladies Lysosomales (VML), Massy France (Agreement N ° 2018-5C) is gratefully acknowledged.

Compliance with ethical standards

Conflict of interest The authors declare that they have no conflict of interest.

Ethical approval All procedures performed in studies involving human participants were in accordance with the ethical standards of the institutional and/or national research committee and with the 1964 Helsinki declaration and its later amendments or comparable ethical standards.

References

1. Ben-Dor, S., Esterman, N., Rubin, E., Sharon, N.: Biases and complex patterns in the residues flanking protein N-glycosylation sites. Glycobiology. **14**, 95–101 (2004)
2. Varki, A., Cummings, R.D., Esko, J.D., Freeze, H.H., Stanley, P., Bertozzi, C.R., Hart, G.W., Etzler, M.E.: Essentials of Glycobiology, 2nd edn. Cold Spring Harbor Laboratory Press, Cold Spring Harbor (NY) (2009)
3. Fuster, M.M., Esko, J.D.: The sweet and sour of cancer: glycans as novel therapeutic targets. Nat. Rev. Cancer **5**, 526–542 (2005)
4. Adamczyk, B., Tharmalingam, T., Rudd, P.M.: Glycans as cancer biomarkers. BBA-Gen. Subjects. **1820**, 1347–1353 (2012)
5. Barone, R., Sturiale, L., Palmigiano, A., Zappia, M., Garozzo, D.: Glycomics of pediatric and adulthood diseases of the central nervous system. J. Proteomics. **75**, 5123–5139 (2012)
6. Kizuka, Y., Kitazume, S., Fujinawa, R., Saito, T., Iwata, N., Saido, T.C., Nakano, M., Yamaguchi, Y., Hashimoto, Y., Staufenbiel, M., Hatsuta, S., Manya, H., Endo, T.: Taniguchi, N.: An aberrant sugar modification of BACE1 blocks its lysosomal targeting in Alzheimer's disease. EMBO Mol. Med. **7**, 175–189 (2015)
7. Palmigiano, A., Barone, R., Sturiale, L., Sanfilippo, C., Bua, R.O., Romeo, D.A., Messina, A., Capuana, M.L., Maci, T., Le Pira, F., Zappia, M., Garozzo, D.: CSF N-glycoproteomics for early diagnosis in Alzheimer's disease. J. Proteomics. **131**, 29–37 (2016)
8. Kizuka, Y., Kitazume, S., Taniguchi, N.: N-glycan and Alzheimer's disease. BBA-Gen Subjects. **1861**, 2447–2454 (2017)
9. Karlsson, I., Ndreu, L., Quaranta, A., Thorsén, G.: Glycosylation patterns of selected proteins in individual serum and cerebrospinal fluid samples. J. Pharmaceut. Biomed. **145**, 431–439 (2017)
10. Delves, P.J.: The role of glycosylation in autoimmune disease. Autoimmunity. **27**, 239–253 (1998)
11. Goulabchand, R., Vincent, T., Batteux, F., Eliaou, J.F., Guilpain, P.: Impact of autoantibody glycosylation in autoimmune diseases. Autoimmun. Rev. **13**, 742–750 (2014)
12. Butler, M., Quelhas, D., Critchley, A.J., Carchon, H., Hebestreit, H.F., Hibbert, R.G., Vilarinho, L., Teles, E., Matthijs, G., Schollen, E., Argibay, P., Harvey, D.J., Dwek, R.A., Jaeken, J., Rudd, P.M.: Detailed glycan analysis of serum glycoproteins of patients with congenital disorders of glycosylation indicates the specific defective glycan processing step and provides an insight into pathogenesis. Glycobiology. **13**, 601–622 (2003)
13. Freeze, H.H.: Genetic defects in the human glycome. Nat. Rev. Genet. **7**, 537–551 (2006)
14. Sparks, S.E.: Inherited disorders of glycosylation. Mol. Genet. Metab. **87**, 1–7 (2006)
15. Sturiale, L., Barone, R., Garozzo, D.: The impact of mass spectrometry in the diagnosis of congenital disorders of glycosylation. J. Inherit. Metab. Dis. **34**, 891–899 (2011)
16. Chang, I.J., He, M., Lam, C.T.: Congenital disorders of glycosylation. Ann. Trans. Med. **6** (2018)
17. Ng, B.G., Freeze, H.H.: Perspectives on glycosylation and its congenital disorders. Trends Genet. **34**, 466–476 (2018)

18. Shubhakar, A., Reiding, K.R., Gardner, R.A., Spencer, D.I., Fernandes, D.L., Wuhrer, M.: High-throughput analysis and automation for glycomics studies. Chromatographia. **78**, 321–333 (2015)
19. Gaunitz, S., Nagy, G., Pohl, N.L., Novotny, M.V.: Recent advances in the analysis of complex glycoproteins. Anal. Chem. **89**, 389–413 (2017)
20. Palmigiano, A., Messina, A., Sturiale, L., Garozzo, D.: Advanced LC-MS Methods for N-Glycan Characterization. In: Cappiello, A., Palma, P. (eds.). Comprehensive Analytical Chemistry Advances in the Use of Liquid Chromatography Mass Spectrometry (LCMS): Instrumentation Developments and Applications. 79, pp. 147–172. Elsevier B.V., Amsterdam (2018)
21. Lauc, G., Essafi, A., Huffman, J.E., Hayward, C., Knezevic, A., Kattla, J.J., Polasek, O., Gornik, O., Vitart, V., Abrahams, J.L., Pucic, M., Novokmet, M., Redzic, I., Campbell, S., Wild, S.H., Borovecki, F., Wang, W., Kolcic, I., Zgaga, L., Gyllensten, U., Wilson, J.F., Wright, A.F., Hastie, N.D., Campbell, H., Rudd, P.M., Rudan, I.: Genomics meets glycomics-the first GWAS study of human N- Glycome identifies HNF1alpha as a master regulator of plasma protein fucosylation. PLoS Genet. **6**, e1001256 (2010)
22. Ruhaak, L.R., Uh, H.W., Beekman, M., Hokke, C.H., Westendorp, R.G., Houwing-Duistermaat, J., Wuhrer, M., Deelder, A.M., Slagboom, P.E.: Plasma protein N-glycan profiles are associated with calendar age, familial longevity and health. J. Proteome Res. **10**, 1667–1674 (2011)
23. Lauc, G., Huffman, J.E., Pucic, M., Zgaga, L., Adamczyk, B., Muzinic, A., Novokmet, M., Polasek, O., Gornik, O., Kristic, J., Keser, T., Vitart, V., Scheijen, B., Uh, H.W., Molokhia, M., Patrick, A.L., McKeigue, P., Kolcic, I., Lukic, I.K., Swann, O., van Leeuwen, F.N., Ruhaak, L.R., Houwing-Duistermaat, J.J., Slagboom, P.E., Beekman, M., de Craen, A.J., Deelder, A.M., Zeng, Q., Wang, W., Hastie, N.D., Gyllensten, U., Wilson, J.F., Wuhrer, M., Wright, A.F., Rudd, P.M., Hayward, C., Aulchenko, Y., Campbell, H., Rudan, I.: Loci associated with N-glycosylation of human immunoglobulin G show pleiotropy with autoimmune diseases and haematological cancers. PLoS Genet. **9**, e1003225 (2013)
24. Ruhaak, L.R., Koeleman, C.A., Uh, H.W., Stam, J.C., van Heemst, D., Maier, A.B., Houwing- Duistermaat, J.J., Hensbergen, P.J., Slagboom, P.E., Deelder, A.M., Wuhrer, M.: Targeted biomarker discovery by high throughput glycosylation profiling of human plasma alpha1-antitrypsin and immunoglobulin A. PLoS One **8**, e73082 (2013)
25. Staples, G.O., Bowman, M.J., Costello, C.E., Hitchcock, A.M., Lau, J.M., Leymarie, N., Miller, C., Naimi, H., Shi, X., Zaia, J.: A chip-based amide-HILIC LC/MS platform for glycosaminoglycan glycomics profiling. Proteomics **9**, 686–695 (2009)
26. Staples, G.O., Naimy, H., Yin, H., Kileen, K., Kraiczek, K., Costello, C.E., Zaia, J.: Improved hydrophilic interaction chromatography LC/MS of heparinoids using a chip with postcolumn makeup flow. Anal. Chem. **82**, 516–522 (2010)
27. Reiding, K.R., Bondt, A., Hennig, R., Gardner, R.A., O'Flaherty, R., Trbojević-Akmačić, I., Shubhakar, A., Hazes, J.M.W., Reichl, U., Fernandes, D.L., Pucic-Bakovic, M., Rapp, E., Spencer, D.I.R., Dolhain, R.J.E.M., Rudd, P.M., Lauc, G., Wuhrer, M.: High-throughput serum N-glycomics: method comparison and application to study rheumatoid arthritis and pregnancy-associated changes. Mol. Cell. Proteomics. **18**, 3–15 (2019)
28. Zhang, T., Madunić, K., Holst, S., Zhang, J., Jin, C., ten Dijke, P., Karlsson, N.G., Stavenhagen, K., Wuhrer, M.: Development of a 96-well plate sample preparation method for integrated N-and O-glycomics using porous graphitized carbon liquid chromatography-mass spectrometry. Mol. Omics. (2020) https://doi.org/10.1039/C9MO00180H
29. Klapoetke, S., Zhang, J., Becht, S., Gu, X., Ding, X.: The evaluation of a novel approach for the profiling and identification of N-linked glycan with a procainamide tag by HPLC with fluorescent and mass spectrometric detection. J. Pharmaceut. Biomed. **53**, 315–324 (2010)
30. Kozak, R.P., Tortosa, C.B., Fernandes, D.L., Spencer, D.I.: Comparison of procainamide and 2-aminobenzamide labeling for profiling and identification of glycans by liquid chromatography with fluorescence detection coupled to electrospray ionization–mass spectrometry. Anal. Biochem. **486**, 38–40 (2015)
31. Lauber, M.A., Yu, Y.Q., Brousmiche, D.W., Hua, Z., Koza, S.M., Magnelli, P., Guthrie, E., Taron, C.H., Fountain, K.J.: Rapid preparation of released N-glycans for HILIC analysis using a labeling reagent that facilitates sensitive fluorescence and ESI-MS detection. Anal. Chem. **87**, 5401–5409 (2015)
32. Kimzey, M., Szabo, Z., Sharma, V., Gyenes, A., Tep, S., Taylor, A., Jones, A., Hyche, J., Haxo, T., Vlasenko, S.: Development of an instant glycan labeling dye for high throughput analysis by mass spectrometry. Prozyme. **25**, 1295 (2015)
33. Zhou, S., Veillon, L., Dong, X., Huang, Y., Mechref, Y.: Direct comparison of derivatization strategies for LC-MS/MS analysis of N-glycans. Analyst. **142**, 4446–4455 (2017)
34. Sturiale, L., Barone, R., Palmigiano, A., Ndosimao, C.N., Briones, P., Adamowicz, M., Jaeken, J., Garozzo, D.: Multiplexed glycoproteomic analysis of glycosylation disorders by sequential yolk immunoglobulins immunoseparation and MALDI-TOF MS. Proteomics. **8**, 3822–3832 (2008)
35. Ceroni, A., Maass, K., Geyer, H., Geyer, R., Dell, A., Haslam, S.M.: GlycoWorkbench: a tool for the computer-assisted annotation of mass spectra of glycans. J. Proteome Res. **7**, 1650–1659 (2008)
36. Rymen, D., Peanne, R., Millón, M.B., Race, V., Sturiale, L., Garozzo, D., Mills, P., Clayton, P., Asteggiano, C.G., Quelhas, D., Cansu, A., Martins, E., Nassogne, M.C., Gonçalves-Rocha, M., Topaloglu, H., Jaeken, J., Foulquier, F., Matthijs, G.: MAN1B1 deficiency: an unexpected CDG-II. PLoS Genet. **9** (2013) https://doi.org/10.1371/journal.pgen.1003989
37. Van Scherpenzeel, M., Timal, S., Rymen, D., Hoischen, A., Wuhrer, M., Hipgrave-Ederveen, A., Grunewald, S., Peanne, R., Saada, A., Edvardson, S., Grønborg, S., Ruijter, G., Kattentidt-Mouravieva, A., Brum, J.M., Freckmann, M.L., Tomkins, S., Jalan, A., Prochazkova, D., Ondruskova, N., Hansikova, H., Willemsen, M.A., Hensbergen, P.J., Matthijs, G., Wevers, R.A., Veltman, J.A., Morava, E., Lefeber, D.J.: Diagnostic serum glycosylation profile in patients with intellectual disability as a result of MAN1B1 deficiency. Brain. **137**, 1030–1038 (2014)
38. Saldova, R., Stöckmann, H., O'Flaherty, R., Lefeber, D.J., Jaeken, J., Rudd, P.M.: N-Glycosylation of serum IgG and total glycoproteins in MAN1B1 deficiency. J. Proteome Res. **14**, 4402–4412 (2015)
39. Duvet, S., Mouajjah, D., Péanne, R., Matthijs, G., Raymond, K., Jaeken, J., Morava, E., Foulquier, F.: Use of endoglycosidase H as a diagnostic tool for MAN1B1-CDG patients. Electrophoresis. 39–3141 (2018)
40. Barbosa, E.A., Fontes, N.D.C., Santos, S.C.L., Lefeber, D.J., Bloch, C., Brum, J.M., Brand, G.D.: Relative quantification of plasma N-glycans in type II congenital disorder of glycosylation patients by mass spectrometry. Clin. Chim. Acta. **492**, 102–113 (2019)
41. Costello, C.E., Contado-Miller, J.M., Cipollo, J.F.: A glycomics platform for the analysis of permethylated oligosaccharide alditols. J. Am. Soc. Mass Spectr. **18**, 1799–1812 (2007)
42. Royle, L., Campbell, M.P., Radcliffe, C.M., White, D.M., Harvey, D.J., Abrahams, J.L., Kim, Y., Henry, G.W., Shadick, N.A., Weinblatt, M.E., Lee, D.M., Rudd, P.M., Dwek, R.A.: HPLC-

based analysis of serum N-glycans on a 96-well plate platform with dedicated database software. Anal. Biochem. **376**, 1–12 (2008)
43. Zhao, P., Peng, X., Luo, S., Huang, Y., Tan, L., Shao, J., He, X.: Identification and characterization of novel mutations in MOGS in a Chinese patient with infantile spams. Neurogenetics. **21**, 97–104 (2020)
44. Sadat, M.A., Moir, S., Chun, T.W., Lusso, P., Kaplan, G., Wolfe, L., Memoli, M.J., He, M., Vega, H., Kim, L.J.Y., Huang, Y., Hussein, N., Nievas, E., Mitchell, R., Garofalo, M., Louie, A., Ireland, D.C., Grunes, C., Cimbro, R., Patel, V., Holzapfel, G., Salahuddin, D., Bristol, T., Adams, D., Marciano, B.E., Hedge, M., Li, Y., Calvo, K.R., Stoddard, J., Justement, J.S., Jacques, J., Priel, D.A.L., Murray, D., Sun, P., Kuhns, D.B., Boerkoel, C.F., Chirini, J.A., Di Pasquale, G., Verthelyi, D., Rosenzweig, S.D.: Glycosylation, hypogammaglobulinemia, and resistance to viral infections. New Engl. J. Med. **370**, 1615–1625 (2014)
45. Jansen, J.C., Timal, S., Van Scherpenzeel, M., Michelakakis, H., Vicogne, D., Ashikov, A., Moraitou, M., Hoischen, A., Huijben, K., Steenbergen, G., van den Boogert, M.A., Porta, F., Calvo, P.L., Mavrikou, M., Cenacchi, G., van den Bogaart, G., Salomon, J., Holleboom, A.G., Rodenburg, R.J., Drenth, J.P., Huynen, M.A., Wevers, R.A., Morava, E., Foulquier, F., Veltman, J.A., Lefeber, D.J.: TMEM199 deficiency is a disorder of Golgi homeostasis characterized by elevated aminotransferases, alkaline phosphatase, and cholesterol and abnormal glycosylation. Am. J. Hum. Genet. **98**, 322–330 (2016)
46. Vajro, P., Zielinska, K., Ng, B.G., Maccarana, M., Bengtson, P., Poeta, M., Mandato, C., D'Acunto, E., Freeze, H.H., Eklund, E.A.: Three unreported cases of TMEM199-CDG, a rare genetic liver disease with abnormal glycosylation. Orphanet J. Rare Dis. **13**, 4 (2018). https://doi.org/10.1186/s13023-017-0757-3
47. Calvo, P.L., Pagliardini, S., Baldi, M., Pucci, A., Sturiale, L., Garozzo, D., Vinciguerra, T., Barbera, C., Jaeken, J.: Long-standing mild hypertransaminasaemia caused by congenital disorder of glycosylation (CDG) type IIx. J. Inherit. Metab. Dis. **31**, 437–440 (2008)
48. Deguchi, K., Keira, T., Yamada, K., Ito, H., Takegawa, Y., Nakagawa, H., Nishimura, S.I.: Two-dimensional hydrophilic interaction chromatography coupling anion-exchange and hydrophilic interaction columns for separation of 2-pyridylamino derivatives of neutral and sialylated N-glycans. J. Chromatogr. A **1189**, 169–174 (2008)
49. Palmisano, G., Larsen, M.R., Packer, N.H., Thaysen-Andersen, M.: Structural analysis of glycoprotein sialylation–part II: LC-MS based detection. RSC Adv. **3**, 22706–22726 (2013)
50. Chantret, I., Dupré, T., Delenda, C., Bucher, S., Dancourt, J., Barnier, A., Charollais, A., Heron, D., Bader-Meunier, B., Danos, O., Seta, N., Durand, G., Oriol, R., Codogno, P., Moore, S.E.: Congenital disorders of glycosylation type Ig is defined by a deficiency in dolichyl-Pmannose: Man-7-GlcNAc2-PP-dolichyl mannosyltransferase. J. Biol. Chem. **277**, 25815–25822 (2002)
51. Thiel, C., Schwarz, M., Hasilik, M., Grieben, U., Hanefeld, F., Lehle, L., von Figura, K., Körner, C.: Deficiency of dolichyl-PMan: Man-7-GlcNAc2-PP-dolichyl mannosyltransferase causes congenital disorder of glycosylation type Ig. Biochem. J. **367**, 195–201 (2002)
52. Grubenmann, C.E., Frank, C.G., Kjaergaard, S., Berger, E.G., Aebi, M., Hennet, T.: ALG12 mannosyltransferase defect in congenital disorder of glycosylation type Ig. Hum. Mol. Genet. **11**, 2331–2339 (2002)
53. Eklund, E.A., Newell, J.W., Sun, L., Seo, N.S., Alper, G., Willert, J., Freeze, H.H.: Molecular and clinical description of the first US patients with congenital disorder of glycosylation Ig. Mol. Genet. Metab. **84**, 25–31 (2005)
54. Di Rocco, M., Hennet, T., Grubenmann, C.E., Pagliardini, S., Allegri, A.E., Frank, C.G., Aebi, M., Vignola, S., Jaeken, J.: Congenital disorder of glycosylation (CDG) Ig: report on a patient and review of the literature. J. Inherit. Metab. Dis. **28**, 1162–1164 (2005)
55. Kranz, C., Basinger, A.A., Gucsavas-Calikoglu, M., Sun, L., Powell, C.M., Henderson, F.W., Aylsworth, A.S., Freeze, H.H.: Expanding spectrum of congenital disorder of glycosylation Ig (CDG-Ig): sibs with a unique skeletal dysplasia, hypogammaglobulinemia, cardiomyopathy, genital malformations, and early lethality. Am. J. Med. Genet. **143A**, 1371–1378 (2007)
56. Murali, C., Lu, J.T., Jain, M., Liu, D.S., Lachman, R., Gibbs, R.A., Lee, B.H., Cohn, D., Campeau, P.M.: Diagnosis of ALG12-CDG by exome sequencing in a case of severe skeletal dysplasia. Mol Genet: Metab. Rep. **1**, 213–219 (2014)
57. Sturiale, L., Bianca, S., Garozzo, D., Terracciano, A., Agolini, E., Messina, A., Palmigiano, A., Esposito, F., Barone, C., Novelli, A., Fiumara, A., Jaeken, J., Barone, R.: ALG12-CDG: novel glycophenotype insights endorse the molecular defect. Glycoconjugate J. **36**, 461–472 (2019)